

# Influence of sulfur on yield and morphology of long carbon nanotubes

© M.A. Khaskov, A.R. Karaeva, E.B. Mitberg, V.Z. Mordkovich

Technological institute for superhard and novel carbon materials of national research centre „Kurchatov institute“, 108840 Troitsk, Moscow, Russia  
e-mail: khaskov@tisnum.ru

Received October 18, 2024

Revised October 18, 2024

Accepted October 18, 2024

The effect of a sulfur-containing activator of carbon nanotube growth on the yield and morphology of the synthesis products obtained by aerosol method of gas-phase chemical vapor deposition was studied at the temperature of 1150°C. Various contents of the sulfur-containing activator in reaction mixtures were used, where the sulfur content was varied in the interval of 0.1–2.0 mass%. The synthesis products were studied by electron microscopy and thermogravimetry. It was shown that the sulfur content affected both the yield and the morphology of the synthesis product obtained, as well as the content of residual catalyst. It was revealed that with a sulfur content of 0.1 to 0.5 mass%, long unidirectional carbon nanotubes prevail in the synthesis products, and with a sulfur content of 0.5 mass%, curved and Y-shaped nanotubes are synthesized. With further increasing of the sulfur content in the reaction mixture, the proportion of unidirectional carbon nanotubes in the products of synthesis is decreased, and „feathered nanotubes“, including spheroidal particles, are appeared. The use of 1.0 mass% or more sulfur in the reaction mixture leads to inhibition of continuous growth of carbon nanotubes with the formation of nanosized clusters of amorphous carbon and graphite-like particles. The results obtained allow us to find the optimal reaction mixture contents for the synthesis of carbon nanotubes with a high yield. It was shown that the presence of sulfur affects the nature of the interaction of carbon and the catalyst particles, while the bond of nanotubes with iron weakens, which favorably affects their growth.

**Keywords:** CNT, carbon nanotubes, nanocomposites, gas-phase chemical vapor deposition, electron microscopy, thermal analysis, growth activator, thiophene.

DOI: 10.61011/TP.2025.02.60833.352-24

## Introduction

Carbon nanotubes (CNT) have a unique combination of properties such as high electrical and thermal conductivity, low density, high strength and corrosion resistance to various corrosive media making them a valuable resource for creating composite materials with vast scope of industrial applications — automotive, aerospace, shipbuilding, modern power engineering and electronics [1–11], etc.

Many properties of CNT-based composite materials depend on the aspect ratio of the carbon filler to be used [12,13], therefore achievement of long CNT and investigation of factors affecting CNT morphology and yield constitute a critical task. One of the methods for obtaining long CNT is suspension catalytic aerosol synthesis by chemical vapor deposition (CVD) [14,15], where volatile sulfur compounds are used as growth promoters [16], and iron-containing compounds are used as a catalyst. Note that the nanotube yield in the total final carbon product obtained by any known CNT synthesis technique is quite low.

Sulfur as the CNT growth promoter plays an important role in increasing the CNT nucleation rate on the catalyst particle surface. Catalyst particles are capable of agglomerating, whereas large particles become inactive and fall into the obtained carbon deposit, thus, increasing the iron content in the obtained CNT [17,18]. Some authors state that sulfur atoms are directly related to the catalyst particle sizes and

have an inhibiting effect on the iron particle agglomeration, while too high content of sulfur reduces the CNT fraction in the synthesis products [19]. Thus, in [20,21], the authors believe that sulfur surrounds iron particles on the surface and separates them from each other thus preventing the agglomeration. In [21], these considerations are supported by the characteristic electron energy loss spectroscopy. On the other hand, in [22], the authors report that sulfur reduces the energy barrier for catalyst particle agglomeration, and the catalyst particle size in the aerosol synthesis of CNT doesn't affect the chemical vapor deposition process during the CNT synthesis. Note that in [21,22], various reagents, i.e. acetone and methane, respectively, were used as a carbon precursor. In case when there are oxygen molecules in the precursor, it may be decomposed to form water that can serve as a carbon matrix oxidizer and shift the sulfur activation mechanism. Thus, contradicting opinions occur in the literature and require experimental investigations for a particular system and CNT synthesis conditions.

The influence of such factors as the nature of carrier gas, ratio of carrier gas and carbon precursor, etc., on the synthesis products was studied earlier in [23], however, the influence of the content of nanotube growth promoter in the reaction gas was not studied.

The objective of this work was to study the influence of the content of sulfur-containing growth promoter in the reaction mixture on the physical and chemical properties

of CNT synthesis products. To achieve the set objective, this study investigated the influence of the concentration of thiophene fed as part of the reactive mixture to the synthesis reactor, where the content of sulfur was varied within 0.1–2.0 mass%, on the yield, morphology, content of residual catalyst and other properties of the CNT synthesis products.

## 1. Experimental

Laboratory system and long CNT preparation technique by aerosol method using chemical deposition from gas-vapor three-component reaction mixture in carrier gas flow are described in earlier works [24]. A flow-type vertical quartz reactor was used. Long CNT synthesis was performed at 1150°C during 1 h in B6.0 grade hydrogen saturated with reaction mixture vapor — ethanol (absolute, C.P. grade, Merck) that was used as a carbon precursor, iron-containing catalyst and sulfur-containing nanotube growth promoter.

Ferrocene (P grade, Merck), 1 mass%, was used as a catalyst. Thiophene (P grade, Merck) was used as a sulfur-containing growth promoter. The sulfur content interval in the reaction mixture was varied within 0.1–2.0 mass%, which corresponded to the thiophene content in the reaction mixture from 0.26 mass% to 5.3 mass%, that was chosen in accordance with the literature data [14] as well as preliminary experimental research data [24]. It should be emphasized that, as opposed to the works of Cambridge University [14] that are considered to be the „pioneers“ in the field of aerosol-based nanotube synthesis by chemical vapor deposition of carbon-containing precursor, reaction mixture was fed into the reactor from bottom to top [25], rather than from top to bottom, to ensure stable nanotube growth and longer residence time in the synthesis zone.

Synthesized CNT in the form of a fibrous „stocking“ were extruded from the synthesis work zone using a rotating spindle into the product receiver on the top of reactor (Figure 1).

Figure 1, right, shows the laboratory setup for long CNT synthesis consisting of three units — gas and reaction mixture vapor feeding unit, reactor unit, and exhaust gas unit. Figure 1, left, shows a photograph of the reactor unit consisting of a high-temperature furnace, quartz reactor and quartz product receiver on the top of the reactor. The product receiver contains a winding device that is used for spindle rotation.

Systematic study and analysis of the prepared long CNT samples were performed by the thermogravimetric analysis (TGA), scanning and transmission electron microscopy (SEM and TEM) methods.

Content of residual iron-containing catalyst in CNT samples was measured thermogravimetrically using the NETZSCH STA 449 F1 simultaneous thermal analyzer (70 ml/min) in dynamic synthetic air at the heating rate of 10 K/min in corundum crucibles with perforated cover. To calculate the content of iron in the samples, a sample

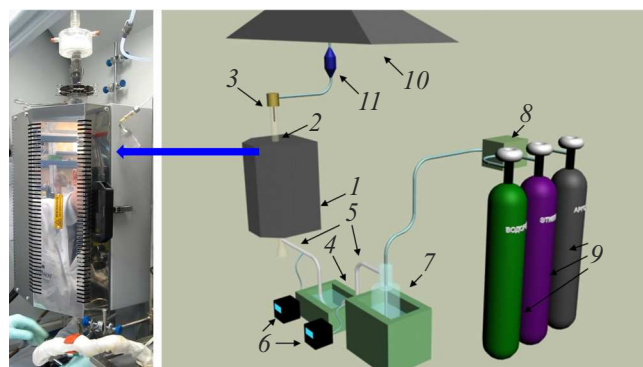


**Figure 1.** Laboratory setup for long CNT synthesis (right), reactor unit photograph (left): 1 — furnace, 2 — quartz reactor, 3 — rotating spindle, 4 — thermostat with ferrocene filled cartridge, 5 — heating strip lines, 6 — heating strip control units, 7 — reaction mixture thermostat, 8 — gas treatment unit (reducers, flow meters, cocks, pressure gauge), 9 — gas bottles, 10 — exhaust fan, 11 — dust collector.

was heated in dynamic synthetic air to complete carbon oxidation and constant weight. The obtained ash residue was multiplied by 0.7, which corresponded to the approximation of the presence of iron in the CNT synthesis products in the form of metallic iron or iron carbides [12] and to complete transformation of iron into iron (III) oxide in the oxidation process during thermoanalytical study.

Morphological features of the CNT samples were studied using the JEOL JSM-7600F high resolution scanning-electron microscope. The microscope is equipped with an energy-dispersive spectrometry (EDS) module with the INCA Energy 350/X-MAX 50 (Oxford Instruments) chemical microanalysis system that is used for local and/or target-area analysis of samples.

The structural features of the CNT samples were examined using the JEOL JEM-2010 transmission electron microscope. Accelerating voltage was 200 kV, line resolution was 0.14 nm.

## 2. Findings and discussion

It is assumed that the long CNT synthesis process in the reactor zone using ferrocene as a catalyst and thiophene as a growth promoter is performed in three steps:

Step I — ferrocene decomposition at 400°C to form iron atoms that collide with each other to produce nanoscale iron clusters [26] and serve later as CNT growth catalysts at high temperatures;

Step II — decomposition of thiophene, sulfur-containing growth promoter. Note that, according to [27], thiophene is decomposed in various temperature ranges following various mechanisms. However, in the presence of iron and during CNT synthesis, decomposition of thiophene starts within 600–800°C [21] releasing sulfur atoms that cover iron nanoclusters and form eutectic phase Fe–S.

Such sulfur coating of iron nanoclusters prevents them from agglomeration (increase in the catalyst size) and increase hydrocarbon solubility in iron;

Step III — decomposition of the carbon source at 700–800°C [21] with release of carbon atoms to form saturated solution with iron atoms and CNT deposition and growth on the solution surface.

Experiments carried out with varying the sulfur content in the reaction mixture within 0.1–2.0 mass% were used to examine the influence of sulfur on the synthesis product yield, morphology and structural features, choose the best sulfur concentration for the long CNT synthesis with the highest yield.

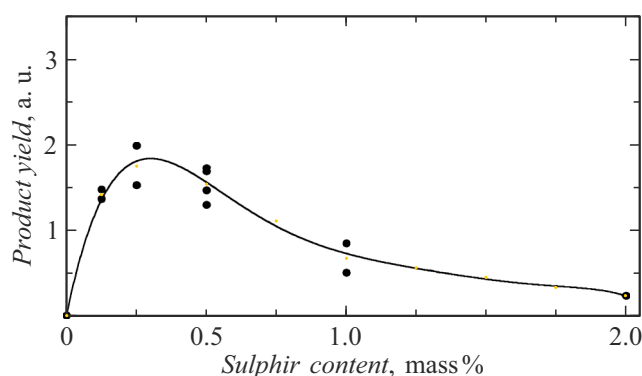
## 2.1. Influence of the sulfur content on the CNT synthesis product yield

Figure 2 shows the curve of CNT synthesis product yield vs. sulfur content.

As shown in Figure 2, the dependence is extremal, where the highest product yield extremum falls into a region with a sulfur content in the reaction mixture of 0.2–0.4 mass%. It can be assumed that at very low sulfur content, less than 0.2 mass%, carbon product formation rate in the reaction mixture decreases and the synthesis time increases to achieve the equal amount of product. With a higher sulfur content, more than 0.4 mass%, carbon product in the reaction mixture is contaminated with sulfur, yield on carbon basis decreases considerably, and the synthesis product becomes less fibrous and harder. When the sulfur content in the reaction mixture is higher than 1.0 mass%, catalytic CNT synthesis is almost reduced to zero, i.e. the catalyst is completely poisoned. Thus, to obtain long CNT with high yield, the optimum sulfur content in the reaction mixture is equal to 0.2–0.4 mass%.

## 2.2. Influence of the sulfur content on the CNT synthesis product morphology and structural features

SEM examinations showed that the morphology of the synthesized CNT depends considerably on the sulfur con-



**Figure 2.** Dependence of the synthesis product yield on the sulfur content in the reaction mixture.

tent in the reaction mixture (Figure 3,4). With a low sulfur content (0.1 mass%), long unidirectional CNT and single agglomerated amorphous and graphite-like carbon particles prevail in the synthesis products (Figure 3, *a*). Increase in the sulfur content in the reaction mixture from 0.2 mass% to 0.4 mass% causes the increase in the yield of long unidirectional CNT (Figure 3, *b*). Curved and Y-shaped CNT occur in the synthesis products with a sulfur content of 0.5 mass% (Figure 4, *a*). With further increase in the sulfur content in the reaction mixture, the fraction of long unidirectional CNT gradually decreases and „finned“ forms of amorphous and graphite-like carbon appear (Figure 4, *b*). Sulfur content of 1.0 mass% and more in the reaction mixture stops the CNT growth completely with formation of nanoscale amorphous carbon clusters and graphite-like carbon particles (Figure 3, *c*).

Note that the TEM samples prepared with the sulfur content of 0.2–0.4 mass% in the reaction mixture demonstrated the prevailing amount of long double-wall CNT. As an example, Figure 5 shows TEM images of both single and bundled double-wall CNT.

SEM and TEM microphotographs of carbon synthesis product samples prepared with the sulfur content of 1.0 mass% in the reaction mixture are shown in Figure 6.

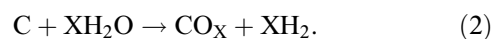
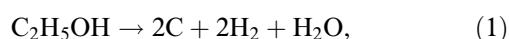
The TEM method showed (Figure 6, *b*) that oval or spheroidal particles on the „finned nanotubes“ or on their tips found by the SEM method (Figure 6, *a*) constitute hollow graphite particles. Figure 6, *b* explicitly shows hollow spheroidal particles.

Carbon synthesis product samples depending on the sulfur content in the reaction mixture are described in the table. Morphology, structural features of samples and CNT bundle diameter were described in accordance with the SEM images, and the Fe content was described from the data obtained by the TGA method.

Thus, with sulfur content in the reaction mixture of 0.25–0.5 mass%, long unidirectional CNT with 9.8–11.4 mass% residual catalyst prevail in the carbon synthesis product.

## 2.3. Influence of the sulfur content on the residual catalyst content in CNT synthesis products

The table shows residual catalyst in synthesis products using different sulfur content in the reaction gas measured by the thermogravimetric analysis method. As shown in the table, iron content correlates with the synthesis product yield on carbon basis and with the content of long unidirectional CNT. Note that the study performed the synthesis using ethanol. In the reaction zone during elimination reaction (equation (1)), ethanol forms water molecules that serve as carbon oxidizer at the synthesis temperatures (equation (2)):





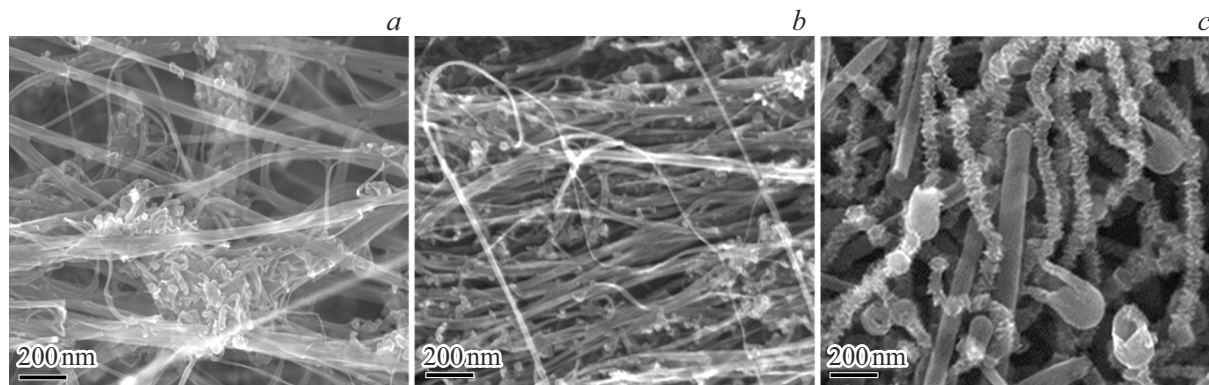


**Figure 3.** SEM images of the CNT samples prepared at different sulfur content values in the reaction mixture: *a* — 0.1, *b* — 0.3, *c* — 1.0 mass% S.

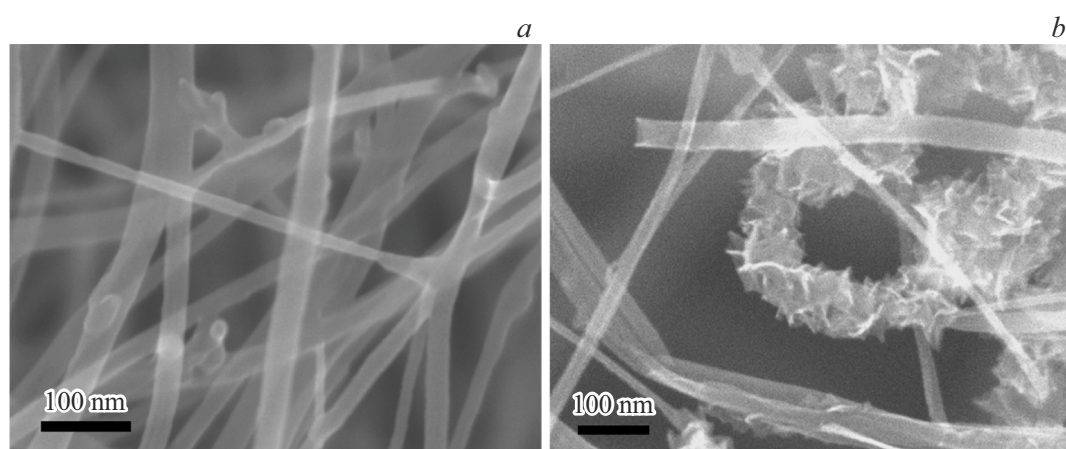


**Figure 4.** SEM images of the CNT samples prepared with the following sulfur content in the reaction mixture: *a* — 0.5, *b* — 0.8 mass% S.

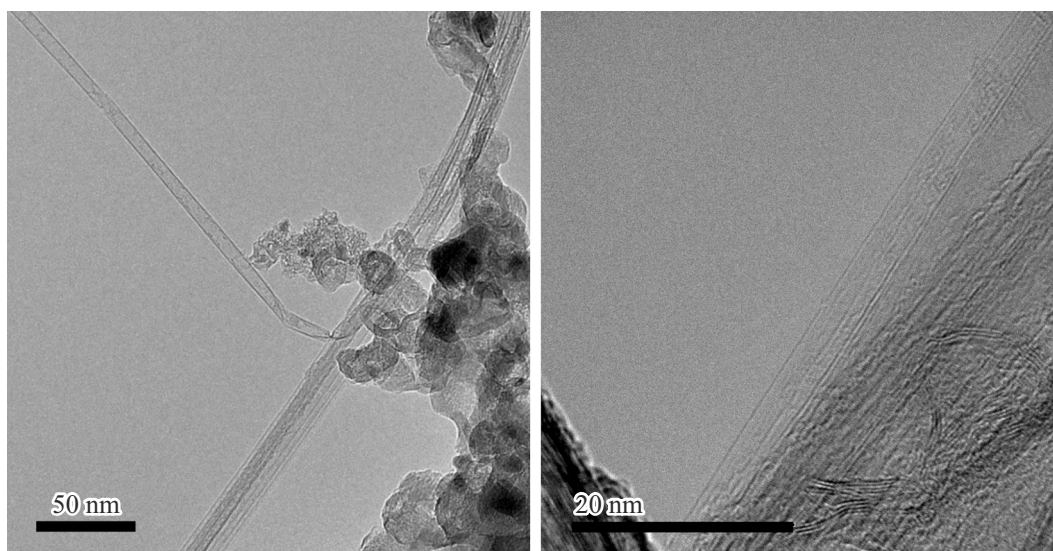


**Figure 5.** TEM images: double-wall long CNT.

According to [28], amorphous and graphite-like carbon has lower thermal-oxidative stability with respect to CNT,

therefore formation of amorphous and graphite-like carbon will presumably facilitate its predominant oxidation by water

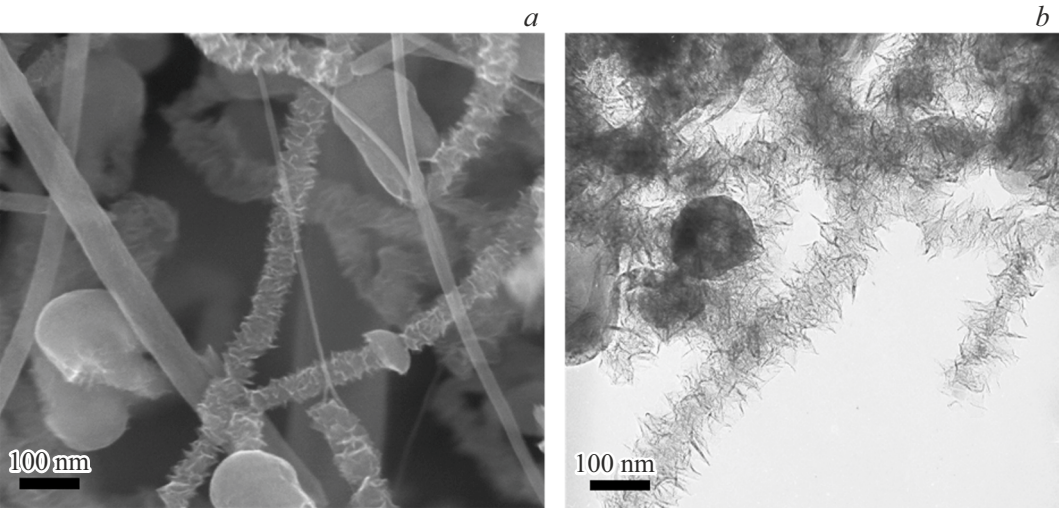


**Figure 6.** Microphotographs of the samples obtained with the sulfur content of 1.0 mass% in the reaction mixture: *a* — SEM image of CNT, „finned nanotubes“, spheroidal particles; *b* — TEM images of „finned nanotubes“, spheroidal particles.

Description of long CNT samples depending on the sulfur content in the reaction mixture						
№	Sulfur content in the reaction mixture, mass%	Description of samples according to SEM images		Visual and–tactile description	Content of Fe, mass%	Yield on carbon basis carbon a.u.
		Morphology and structural features	CNT bundle diameter, nm			
1	0.1–0.2	Straight unidirectional CNT bundles and single agglomerated amorphous graphite-like carbon particles	10–40	Sticky, fibrous, less dense	4.2–5.2	1.3–1.5
2	0.25–0.5	Unidirectional CNT prevail, there are curved and Y-shaped legs about 20 nm in diameter, branched of straight nanotubes, there are also agglomerated amorphous and graphite-like carbon particles	7–35	Sticky, fibrous, denser	9.8–11.4	1.2–2.0
3	0.8–1.0 and more	„Finned nanotubes“ prevail. There are single straight nanotubes and oval or spheroidal particles about 100 nm in size, located on „finned nanotubes“	6–60	Non-sticky, non-fibrous, loose	0.2–0.5	0.1–0.8

molecules to form volatile carbon oxides and will not give rise to solid carbon product and thus will be characterized by zero yield on carbon basis. The obtained data confirms that iron is a key element for CNT formation in the experiment conditions, whereas sulfur content variation presumably facilitates the variation of catalytic activity with its maximum at the sulfur content in the reaction mixture within 0.2–0.4 mass%.

Thus, the findings show that sulfur exerts a significant impact both on the yield and morphology of the product.

The literature proposes several models describing the role of sulfur in the catalytic growth of nanotubes. For example, according to [29], sulfur is deposited on the surface of catalyst particles and, with the optimum filling of active centers, is the growth promoter of Y-shaped nanotubes, and completely poisons the catalytic capacity of nanotube synthesis when the degree of filling is even greater. The results of the experiments and study suggest that, with low filling of catalytic centers, sulfur on the catalyst particle promotes the growth of unidirectional CNT,

which explains the observed shape of curve in Figure 2. On the other hand, according to [30], the presence of sulfur in catalytic CNT growth gives rise to nanotube growth branching processes, five-membered and seven-membered carbon cycles, thus, increasing the presence of Y-shaped nanotubes and amorphous carbon. In our case, this is probably the reason for the loss of „stickiness“ and fibrousness of carbon deposit samples as the sulfur content in the reaction mixture increases.

Thus, the findings suggest that, when the thiophene content in the reaction mixture is low, lower than 0.2 mass%, sulfur precipitates on the catalyst particle surface, promotes the growth of aligned unidirectional nanotubes, with optimum (0.2–0.4 mass%) filling of active catalyst centers, sulfur activates the growth of not only aligned unidirectional nanotubes, but also Y-shaped ones (0.4–0.5 mass%), and, when the degree of filling is even greater (1.0 mass%), completely poisons the catalytic activity of iron particles, and the nanotube synthesis stops.

## Conclusion

The study investigated the impact of sulfur-containing component, thiophene, fed into the synthesis reactor as part of the reaction mixture on the yield and morphology, and also other properties of long CNT synthesis products. It is shown that sulfur has a significant impact on the carbon yield in the chemical vapor deposition reaction of ethanol using the aerosol method as well as on the morphology of the product and content of residual iron catalyst in it.

Results of the study made it possible to find the optimum content of sulfur within 0.2–0.4 mass% to obtain long CNT with high yield. Formation of single branched Y-shaped nanotubes with the sulfur content of 0.4–0.5 mass% was a side effect. It is shown that low content of sulfur in the reaction mixture (lower than 0.2 mass%) gives rise to the growth of aligned unidirectional nanotubes, but with low yield. Excess sulfur content in the reaction mixture poisons the catalytic activity of iron particles and long CNT synthesis stops. Non-catalytic synthesis gives rise to a large amount of amorphous and graphite-like product in the form of „fanned nanotubes“ with oval or spheroidal graphite particles.

## Acknowledgments

The authors are grateful to the structural research department team of the National Research Center „Kurchatov Institute“ — Technological Institute for Superhard and Novel Carbon Materials - N.I. Batova and B.A. Kulnitsky for electron microscopic examinations.

## Funding

This study was supported under state assignment of 2025.

## Conflict of interest

The authors declare no conflict of interest.

## References

- [1] S. Yang. *Archit. Struct. Constr.*, **3**(3), 289 (2023). DOI: 10.1007/s44150-023-00090-z
- [2] A.K. Jagadeesan, K. Thangavelu, V. Dhananjeyan. *Publish with Intech Open*, (2020). DOI: 10.5772/intechopen.92995
- [3] S. Abdalla, F. Al-Marzouki, A.A. Al-Ghamdi, A. Abdel-Daiem. *Nanoscale Res Lett.*, **10**(1), 358 (2015). <https://doi.org/10.1186/s11671-015-1056-3>
- [4] M.F. De Volder, S.H. Tawfick, R.H. Baughman, A.J. Hart. *Science*, **339**(6119), 535 (2013). DOI: 10.1126/science.1222453
- [5] E. Muchuweni, E.T. Mombeshora, B.S. Martincigh, V.O. Nyamori. *Front. Chem.*, **9** (2022). DOI: 10.3389/fchem.2021.733552
- [6] A. Venkataraman, V.A. Eberchukwu, Y. Chen, C. Papadopoulos. *Nanoscale Res. Lett.*, **14**(1), 220 (2019). DOI: 10.1186/s11671-019-3046-3
- [7] N. Gupta, S.M. Gupta, S.K. Sharma. *Carbon Lett.*, **29**, 419 (2019). DOI: 10.1007/s42823-019-00068-2
- [8] R. Rao, C.L. Pint, A.E. Islam, R.S. Weatherup, S. Hofmann et al. *ACS Nano*, **12**(12), 11756 (2018). DOI: 10.1021/acsnano.8b06511
- [9] M. Trivedi, Reecha. *Chem. Sci. Rev. Lett.*, **9**(33), 1 (2020). DOI: 10.37273/chesci.CS20510188
- [10] K. Cui, J. Chang, L. Feo, C.L. Chow, D. Lau. *Front. Mater.*, **9** (2022). DOI: 10.3389/fmats.2022.861646
- [11] D. Liu, L. Shi, Q. Dai, R. Mehmood, Z. Gu, L. Dai. *Trend Chem.*, **6**(4), 186 (2024). DOI: <https://doi.org/10.1016/j.trechm.2024.02.002>
- [12] V.Z. Mordkovich, M.A. Khaskov, V.A. Naumova, V.V. De, B. Kulnitskiy, A.R. Karaeva. *Compos. Sci.*, **7**(2), (2023). DOI: 10.3390/jcs7020079
- [13] J. Chen, L. Yan. *Fullerenes, Nanotubes and Carbon Nanostructures*, **26**(11), 697 (2018). DOI: 10.1080/1536383X.2018.1476345
- [14] Y.-L. Li, I.A. Kinloch, A.H. Windle. *Science*, **304**, 276 (2004). DOI: 10.1126/science.1094982
- [15] A.R. Karaeva, N.V. Kazennov, E.A. Zhukova, V.Z. Mordkovich. *Mater. Today*, **5**(12), 25951 (2018). DOI: 10.1016/j.matpr.2018.08.010
- [16] B. Orbán, T. Höltzl. *Dalton Trans.*, **51**, 9256 (2022). DOI: 10.1039/d2dt00355d
- [17] D. Conroy, A. Moisala, S. Cardoso, A. Windle, J. Davidson. *Chem. Eng. Sci.*, **65**(10), 2965 (2010). DOI: 10.1016/J.CES.2010.01.019
- [18] D. Janas, K.K. Koziol. *Nanoscale*, **8**(47), 19475 (2016). DOI: 10.1039/c6nr07549e
- [19] V. Reguero, B. Aleman, B. Mas, J.J. Vilatela. *Chem. Mater.*, **26**, 3550 (2014). DOI: 10.1021/cm501187x
- [20] R.M. Sundaram, K.K. Koziol, A.H. Windle. *Adv. Mater.*, **23**(43), 5064-8 (2011). DOI: 10.1002/adma.201102754
- [21] S.-H. Lee, J. Park, H.-R. Kim, J. Lee, K.-H. Lee, *RSC Adv.*, **5**, 41894 (2015). DOI: 10.1039/C5RA04691B
- [22] C. Hoecker, F. Smail, M. Pick, L. Weller, A.M. Boies. *Sci. Rep.*, **7**, 14519 (2017). DOI: 10.1038/s41598-017-14775-1

- [23] M.A. Khaskov, A.R. Karaeva, V.N. Denisov, B.A. Kultitskiy, V.Z. Mordkovich. Chem. Chem. Tech., **56** (7), 76 (2013).
- [24] A.R. Karaeva, M.A. Khaskov, E.B. Mitberg, B. Kulnitskiy, I.A. Perezhogin, L. Ivanov, V. Denisov, A. Kirichenko, V. Mordkovich. Fuller. Nanotub. Carbon Nanostruct., **20** (4–7), 411 (2012). DOI: 10.1080/1536383X.2012.655229
- [25] A.R. Karaeva, S.A. Urvanov, N.V. Kazennov, E. Mitberg, V. Mordkovich. Nanomaterials, **10** (11), 2279 (2020). DOI: 10.3390/nano10112279
- [26] A. Bhattacharjee, A. Rooj, D. Roy, M. Roy. J. Exper. Phys., **2014**, Article ID 513268 (2014). DOI: 10.1155/2014/513268
- [27] S. Xian, Q. Xu, H. Li. ACS Omega, **8** (37), 33982 (2023). DOI: 10.1021/acsomega.3c04847
- [28] M.A. Khaskov. Chem. Chem. Tech., **66** (10), 24 (2023). DOI:10.6060/ivkkt.20236610.1y
- [29] H. Zhu, L. Ci, C. Xu, J. Liang, D. Wu. Diamond and Related Mater., **11** (7), 1349 (2002). DOI: 10.1016/S0925-9635(01)00745-2
- [30] J.M. Romo-Herrera, B.G. Sumpter, D.A. Cullen, H. Terrones, E. Cruz-Silva, D.J. Smith, V. Meunier, M. Terrones. Angew. Chem. Int. Ed., **47** (16), 2948 (2008). DOI: 10.1002/anie.200705053

*Translated by E.Ilinskaya*